PROCEEDINGS, 49th Workshop on Geothermal Reservoir Engineering
Stanford University, Stanford, California, February 12-14, 2024
SGP-TR-227

Updating Fault Model with using Borehole Image Data on Patuha Geothermal System, West Java, Indonesia

Ezidin Reski, Yuris Ramadhan, And Randy Wijaya Atmaja

ezidin@geodipa.co.id; yuris.r@geodipa.co.id; randy@geodipa.co.id

Keywords: Structural geology, fractures, bore hole image, permeability, Patuha

ABSTRACT

Patuha geothermal field is a steam-dominated geothermal system lying on a quaternary volcanic unit in West Java Province, Indonesia. The fault structure and rock deformation in Patuha may strongly control the permeability and being a media to generate the steam production in the wellbore. Geodipa has conducted a structure study prior to the drilling campaign and the updated one will be presented through this paper which aimed to reevaluate the surface geological structure framework from the interpretation from borehole image data to improving well targeting.

The geological structure framework analysis from LiDAR data, fieldwork measurement, and review some of the subsurface data such as feedzones and MeQ were done on 2023. The result was showing a strike-slip system developed in the larger Patuha area with the main fault trending NE-SW, while the accompanying fault is en-echelon faults trending relatively NNE-SSW The model also will explain the link between the larger tectonic framework and the detailed structure model scale in Patuha.

Later, when the interpretation from borehole image data was done, it shows the comprehensive fracture trend in detail scale. The result so far confirming the presence of NW-SE trend on 2 wells but also show NNE-SSW trends that is parallel with our current stress interpretation. The data also confirming the high dip angle fault that align with strike slip system fault model that been developed earlier. In conclusion, these result so far has been contributed and improved the geological structure interpretation's confidence for well targeting and provide a confirmation of general fracture trend associated with surface fault to predict permeable zone area.

1. INTRODUCTION

The Patuha Geothermal Field is located in West Java, about 50 kilometers southwest of Bandung. The field is situated within a northwest-trending volcanic mountains range, such as Mt. North Patuha, Mt. South Patuha, Mt. Urug, Mt. Puncaklawang, Mt. Pungkur, and other surrounding peaks (Ashat et. al., 2019). Surface thermal manifestations distributed in Patuha field are fumaroles at K. Putih, K. Cibuni, and K. Ciwidey, thermal springs are located on the south, west, and northwest flank of the volcanic highland (**Figure 1**).

Previous structural interpretation was conducted in 2016 (Pradipta, 2016), 2020-2021 prior to drilling campaign (Chandra et. al., 2022) and 2023 updated during Patuha's drilling campaign shown in **Figure 2**. The latest structure accommodated tectonic regimes on a larger **S**cale and it correspond to the deformation history of field-scale structures (**Figure 3**). However, the latest structure model not supported yet with bore hole image data to make robust interpretation.

The current focus of study was concentrated on fault confirmation using bore hole image data and integrated with surface fault. This confirmation is important part to asses Patuha's productive permeability fault.

In 2023, several new wells were drilled in Patuha geothermal field from which image logs were collected. We compare observations of drilling events, occurrence of natural fractures, and feed zones, and highlight their correspondence.

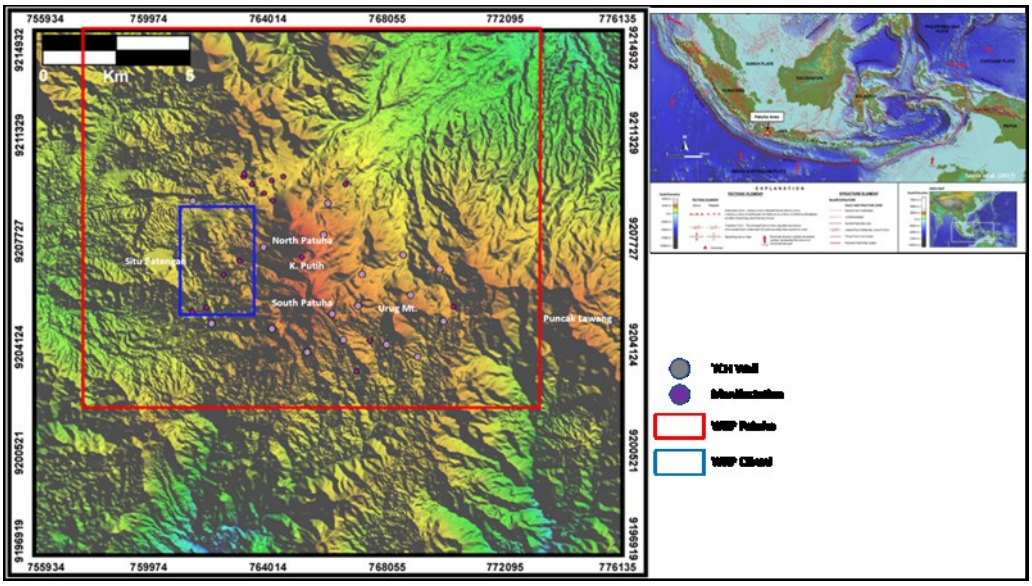

Figure 1: Patuha field location with Digital Elevation Model (DEM) from LiDAR as background

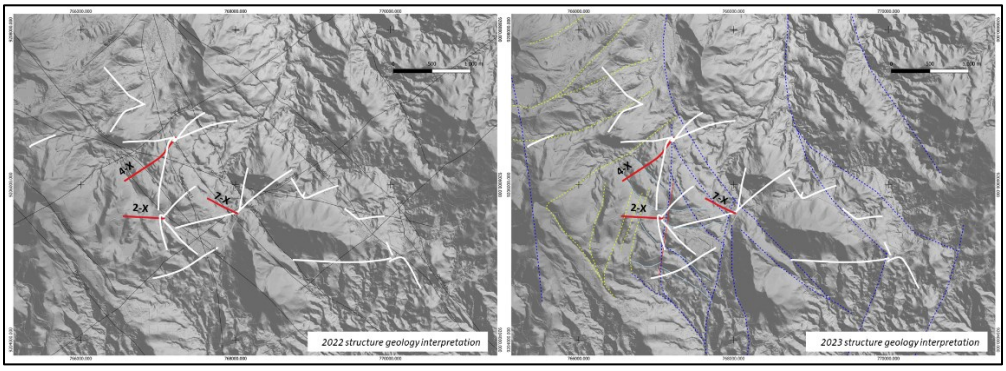

Figure 2. Patuha Updated structure geology interpretation

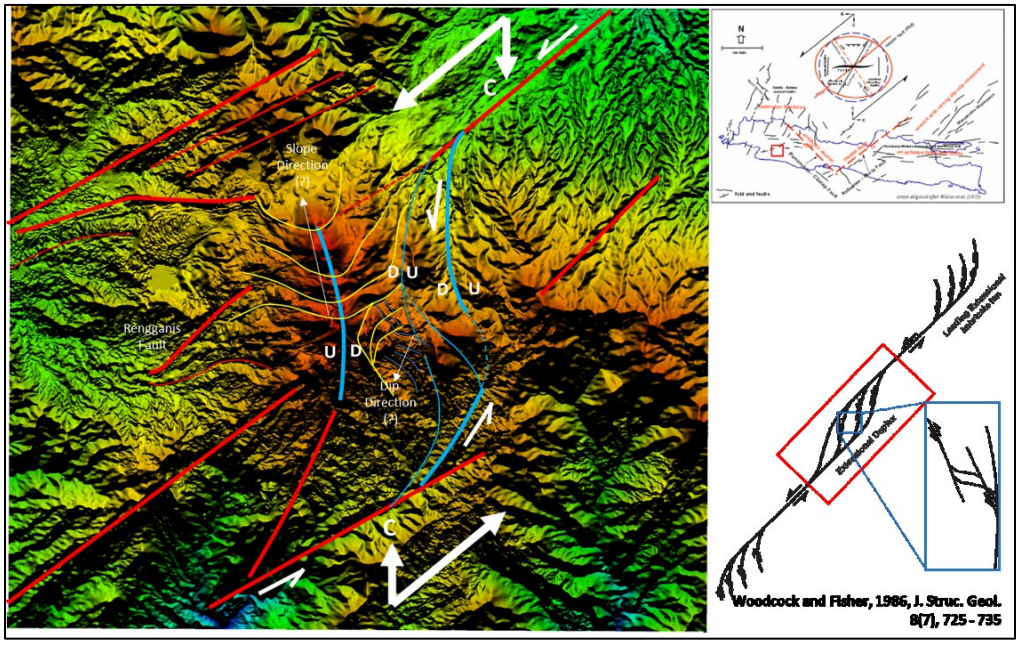

Figure 3. Patuha Structure Geology Framework Model

2. GEOLOGICAL SETTING

The surface geology of Patuha boasts a rich tapestry of 25 distinct volcanic units, each bearing witness to the region's fiery past. Building upon this primary data, the interpretation incorporates valuable insights from earlier investigations by Kusdji (2013) and unpublished research by Pusat Penelitian Panas Bumi FTUGM (2020). Previous studies divided the subsurface rocks into eight stratigraphic units: Puncakkopsi, Puncaklawang, Kendeng, Tikukur, Patuha, Sugihmukti, Urug, and Malabar. This division was based on the characteristics and spatial association of these units with the surface volcanic products. Examination of primary data and previous studies revealed that the Patuha field's subsurface stratigraphy predominantly comprises Quaternary andesitic-dacitic lava, pyroclastic rocks, and diorite. Petrographic analysis further classified these rocks into three primary groups. Andesitic Lava characterized by the presence of plagioclase and pyroxene within a groundmass of microcrystalline plagioclase and glass, these rocks constitute the Puncaklawang products, found at the lowermost volcanic sequence. Dacitic Lava comprising plagioclase, quartz, and pyroxene phenocrysts embedded in a groundmass of similar mineralogy and minor volcanic glass, these rocks are abundant in the field. They form the Patuha Tua and Urug products, with the Patuha Tua sequence being the most widespread. Pyroxene Andesitic Lava defined by the presence of plagioclase, pyroxene, hornblende, and trace amounts of biotite in a groundmass of microcrystalline plagioclase, pyroxene, and clay minerals, this lava type belongs to the Sugihmukti 1 product. Diorite identified at depths exceeding 1,000 meters, diorite comprises primary minerals like plagioclase and quartz, accompanied by minor pyroxene and hornblende, all embedded within microcrystalline crystals of similar mineralogy.

3. REGIONAL TECTONIC SETTING

Patuha's geothermal field is located at the southern tip of Java Island, the oceanic crust of the Indo-Australian Plate plunges beneath the continental crust of the Eurasian Plate at a rapid rate of 6-7 cm/year in a N20°E direction (Pulunggono et al., 1994). This violent process of subduction releases immense heat, creating potential geothermal reservoirs where Patuha lies. West Java's tectonic history has left its mark on the region's structural configuration. Three dominant sets of trends have been identified, N-S Sunda Trend with north-south alignment reflects the influence of the Sunda Arc and its associated collision zone. Sribudiani et al. 2003 mention that NE-SW Meratus Trend with trend originates from the Meratus Ridge subduction system further east and E-W Java Trend with east-west direction reflects the regional stress field associated with plate motions **(Figure 4)**. Satyana (2007) have recognized the strong influence of NE-SW, NW-SE, and E-W trends on the regional tectonic setting of West Java. These trends, mirroring the various phases of subduction, further reinforce the connection between tectonic activity and geothermal resources. Current horizontal stress maps showcase a dominant NE-SW trend, paralleling the absolute plate motion directions (Stingay et al., 2010). This alignment suggests that ongoing subduction continues to influence the present-day tectonic landscape and likely contributes to the localization of geothermal potential in Patuha. Studies by Elfina et al. (2017) reveal a layered subsurface structure within the Patuha field, further influenced by local tectonic events. These layers, characterized by varying permeability and temperature, control the flow and distribution of geothermal fluids within the reservoir. Understanding this internal architecture is crucial for optimizing reservoir management and ensuring the long-term sustainability of the field.

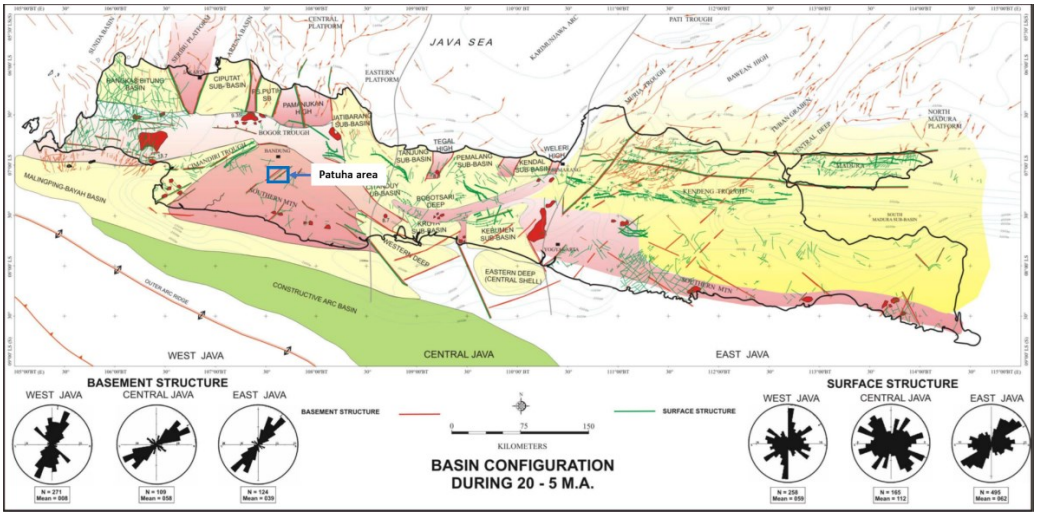

Figure 4. Tectonic framework of Java Island at 20 – 5 Ma (Sribudiani et al. 2003)

4. DRILLING RECORD

4.1 Lithology and drilling cutting

Information from cuttings is considered unreliable in reservoir section due to using aerated water when TLC was encountered. In reservoir section during cutting return, lithology observed are interplayed fine tuff and coarse pyroclastic and predominantly andesite at bottom of 12¼" hole section. Based on the results of megascopic analysis of drill cuttings, lithological sequence is composed of andesite, lithic to crystal coarse pyroclastic, lithic tuff and fine-grained crystal tuff with mostly has propylitic alteration type. This type of alteration characterized by the lack of low temperature clay minerals and presence of high temperature altered minerals such as Chlorite, Anhydrite and Epidote (**Figure 5**). In this study, quantitative analysis revealed a significantly higher intensity of fractures within coarse pyroclastic rocks compared to both andesite and fine pyroclastic formations. This suggests that coarse pyroclastic rocks are more likely to form

fractures when subjected to stress. In 2-X and 7-X well section, the presence of a drilling break followed by TLC emerged as a highly reliable preliminary indicator for identifying fracture-related feedzones. This observation provides valuable insights for targeted exploration efforts aimed at locating reservoirs associated with fractured zones within pyroclastic sequences. Further studies are warranted to quantitatively assess the influence of grain size and clast composition on fracture development within pyroclastic deposits. Integrating these findings with geomechanical modelling could enhance the prediction and characterization of potential reservoir compartments in fractured pyroclastic reservoirs.

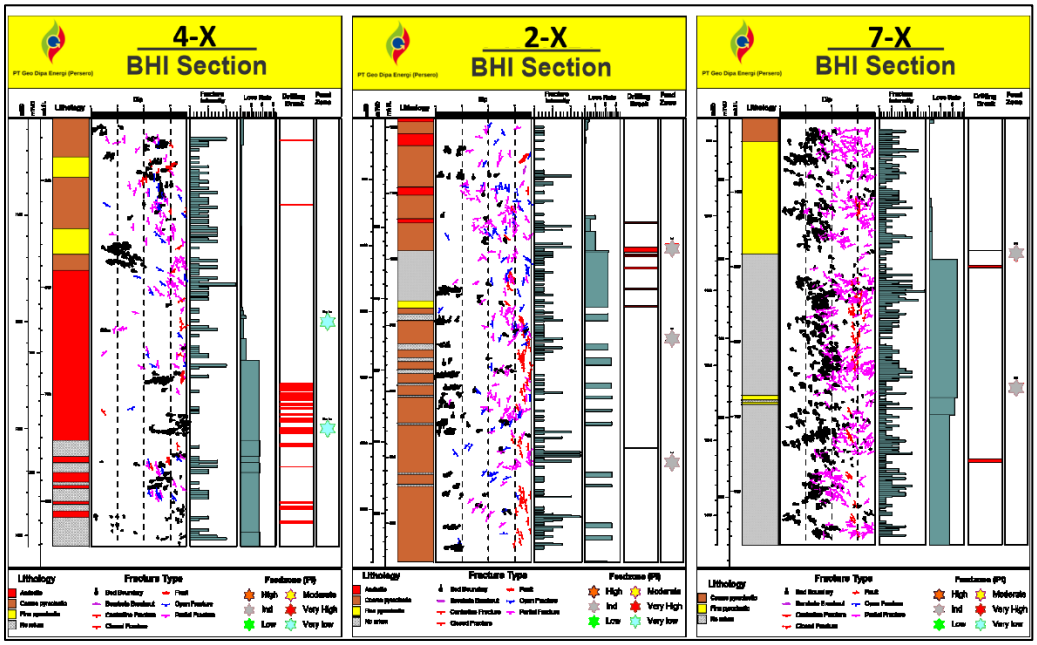

Figure 5. Lithological column

4.2 Permeability Indication During Drilling

Permeability in Patuha area is indicated based on integrating data from the loss zones, drilling parameters (drilling break), formation imaging log, and the completion test, Feedzone in 4-X and 2-X well was already confirmed by discharge test, while 7-X well can be indicate by injection test only. Overall, the distribution and nature of permeability encountered is consistent with it being predominantly structurally controlled

During drilling in reservoir zone, total loss circulation All the produced drilling cuttings from this well were returned to the surface by underbalanced drilling complete with foam and synthetic polymer. Drilling fluid was already improved to manage loss circulation at the top section and at the reservoir section (**Table 1**).

Table 1. Permeability Indication During Drilling

Well ID	Drilling Break	Drilling Loss		Feedzone
	Depth	Depth	Type	Depth
4-X		810 - 1311	PLC	
	1276 - 1279			1200
	1280 - 1282			
	1286 - 1288			
	1290 - 1294			
	1299 - 1305			1300
	1314 - 1317	1311 - 1326	TLC	
	1333.9 - 1334	1326 - 2036	Intermittent	
	1335.9 - 1336			
	1368 - 1370			
	1372 - 1376			
	1386 - 1389			
	1484.5 - 1485			
	1498 - 1501			
	1607 - 1612			1650
	1681 - 1685			
	1759 - 1761			
	1862 - 1863			
	1871 - 1872			
	1965 - 1966			1900
	1967 - 1968			
	1981 - 1982			

Well ID	Drilling Break	Drilling Loss		Feedzone
	Depth	Depth	Type	Depth
2-X		810 - 1008	PLC	
	1003 - 1010	1008 - 1580	Intermittent - TLC	1005
	1013.5 - 1015			
	1015.7 - 1017.4			
	1033 - 1036			
	1066 - 1067			
	1092 - 1093			1141
	1307 - 1307			1329

Well ID	Drilling Break	Drilling Loss		Feedzone
	Depth	Depth	Type	Depth
7-X		843 - 1059	PLC	
	1046 - 1047	1059 - 1243	TLC	1050
	1066 - 1069			
		1243 - 1428	Intermittent - TLC	1230
	1325 - 1330			
	1473 - 1475			1499.5
	1569 - 1572			

4.3 Bore Hole Image

High-resolution image logging utilizing a BHPT-XRMI tool in 12¼" open hole sections revealed the subsurface lithology at wells 4-X, 2-X, and 7-X. Consistent with geological predictions, the dominant formations were identified as pyroclastic and andesites, corroborating wellsite geological logging and petrographic analyses. Overall data quality from the image logs was generally excellent, enabling detailed fracture network characterization. However, specific intervals exhibited borehole rugosity challenges, necessitating careful feature identification and interpretation.

A comprehensive fracture analysis was conducted through manual dip picking and classification of identified features into foliation/joints, fractures, and linear features. This analysis yielded significant fracture populations within each well: 403 fractures in 4-X (1015-1408 mMD), 459 fractures in 2-X (808.5-1470 mMD), and 421 fractures in 7-X (884-1427 mMD).

4.3.1 4-X Image interpretation

High-resolution image logging of 4-X well section unveils a multifaceted fracture network with distinct directional patterns (**Figure 6** and **Figure 7**). Open fractures, crucial for geothermal fluid flow, exhibit a dominant NW-SE trend concentrated between N330°E and N360°E, suggesting valuable targets for future well placement. Interestingly, resistive fractures and bed boundaries follow an ENE-WSW trend, hinting at potential reservoir compartmentalization. This dual orientation system, accompanied by dips ranging from 70° to 90°, paints a detailed picture of the subsurface fracture network.

Furthermore, drilling-induced fractures aligned with the NE-SW direction corroborate the maximum horizontal stress orientation. While absent in this section, borehole breakouts underscore the importance of accurate stress modeling for deviated wells to ensure trajectories intercepting productive fracture zones. Estimated apertures for conductive fractures range from 0.00mm to 1.14mm with a mean of 0.39mm, further supporting the presence of high-angle faults confirmed by the 2023 fault model (**Figure 8**).

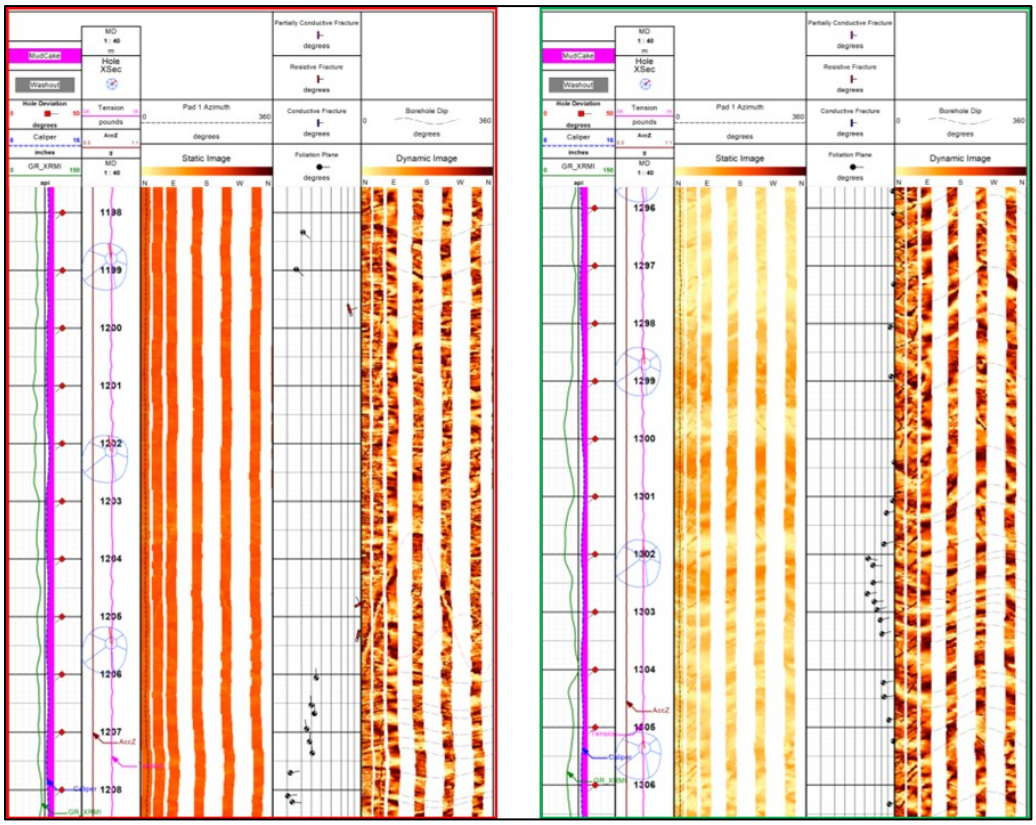

Figure 6. 4-X fractures identified from the image log

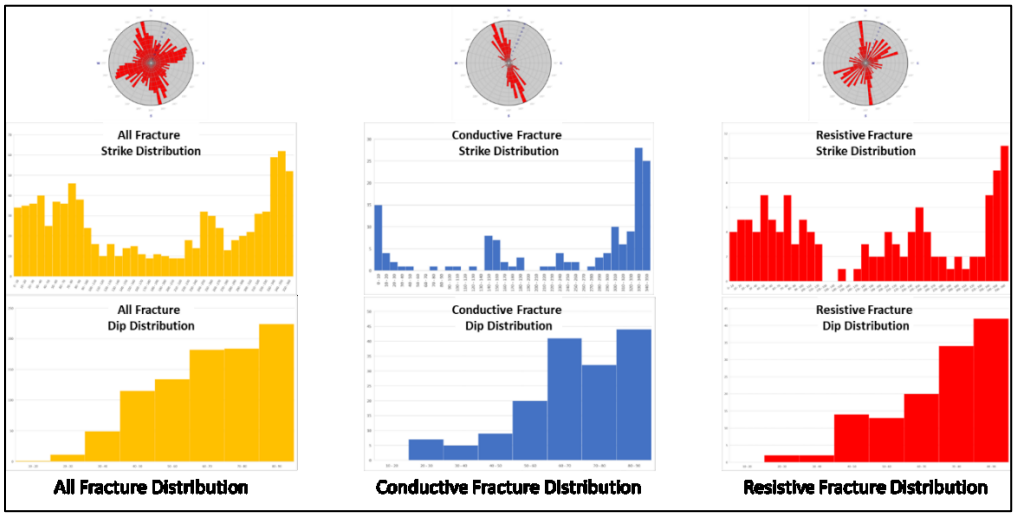

Figure 7. 4-X fracture distribution

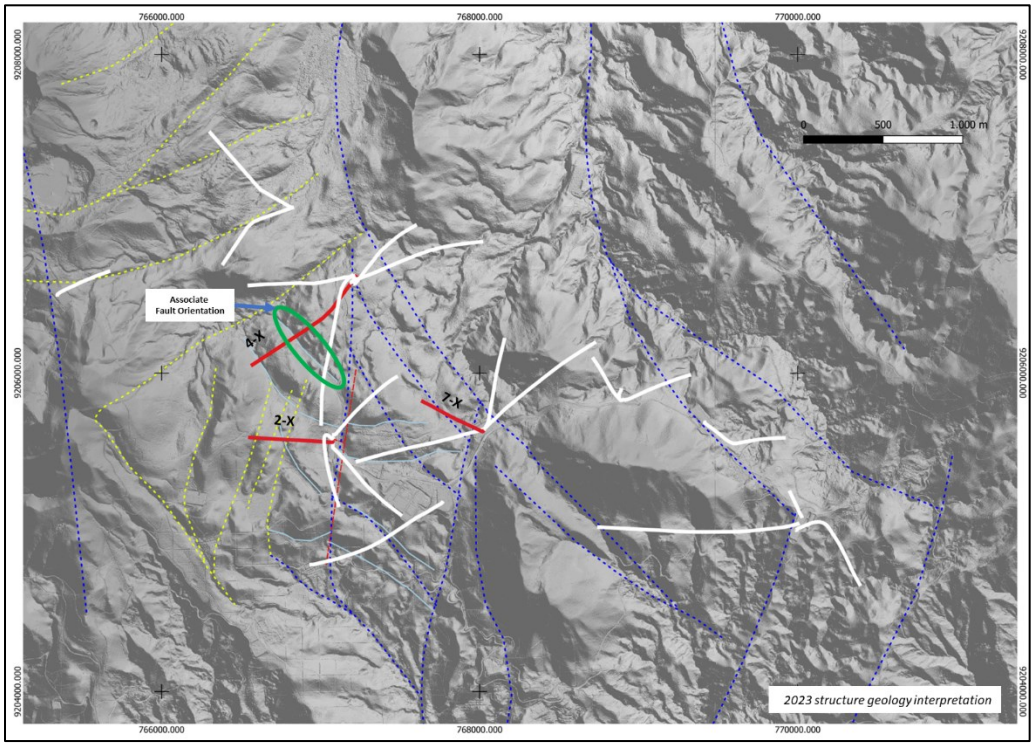

Figure 8. 4-X fault associate

4.3.2 2-X Image interpretation

High-resolution image logging of 2-X reveals a complex fracture network with distinct directional patterns (**Figure 9** and **Figure 10**). Partially conductive fractures dominate the system, exhibiting preferential orientations in both relative N-S and NE-SW directions. Open fractures, crucial for fluid flow in geothermal reservoirs, primarily follow these trends, concentrated between N30-50°E and N340-360°E with dip angle ranging from 70° to 90°. This dual orientation system suggests potential preferential pathways for geothermal fluids and highlights the importance of targeting wells accordingly.

Drilling-induced linear features are observed primarily in the East-West direction, aligning with the maximum horizontal stress orientation. However, due to incomplete borehole coverage, their interpretation needs caution as in-situ stress indicators. The absence of evident borehole breakout features further underscores the need for accurate stress modeling, particularly for deviated wells, to ensure optimal well trajectories intercepting productive fracture zones. Estimated apertures for conductive fractures range from 0.381mm to 0.77mm, while partially conductive fractures exhibit apertures between 0.3mm and 0.9mm (mean and maximum values, respectively),

further supporting the presence of potentially transmissive fracture networks. These findings, corroborated by the 2023 fault model **(Figure 11**), provide valuable insights for optimizing geothermal well targeting in Patuha area**.**

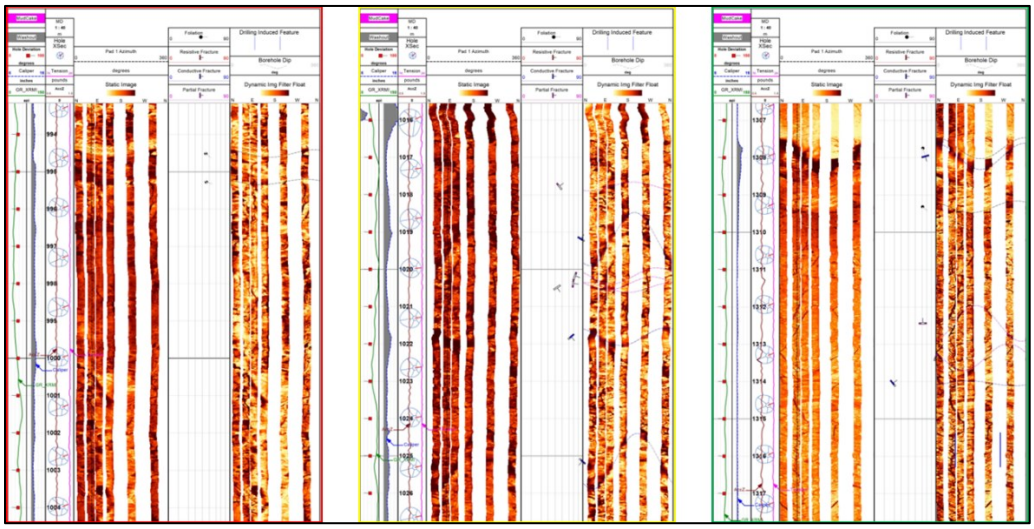

Figure 9. 2-X fractures identified from the image log

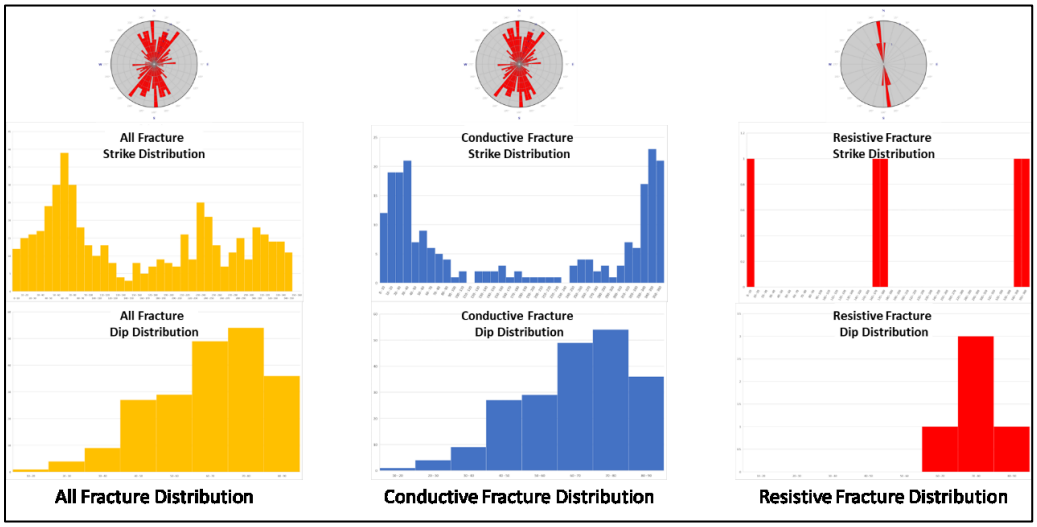

Figure 10. 2-X fracture distribution

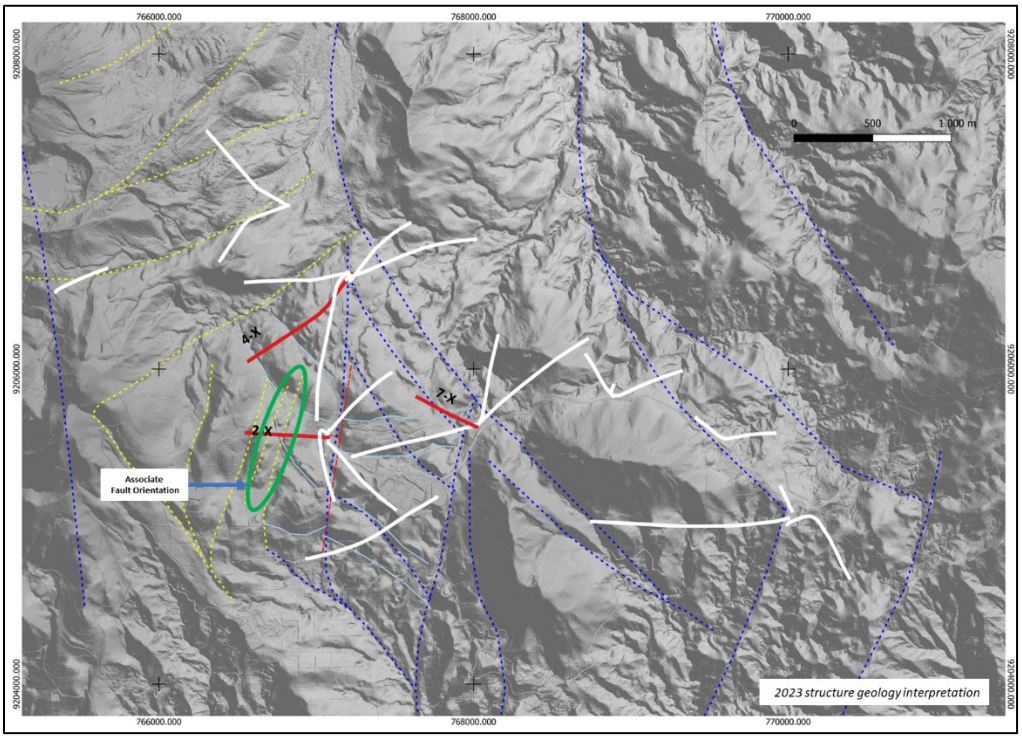

Figure 11. 2-X fault associate

4.3.3 7-X Image interpretation

High-resolution image logging of 7-X reveals a complex fracture network with distinct directional patterns (**Figure 12** & **Figure 13**). Partially conductive fractures dominate the system, exhibiting a preferential orientation in the relative WNW-ESE direction. However, open fractures, crucial for fluid flow in geothermal reservoirs, follow a different trend, aligning primarily with relative N-S and NE-SW directions concentrated between N30-50°E and N340-360°E with steep dips ranging from 70° to 90°.

This contrasting orientation pattern suggests the presence of multiple fracture sets within 7-X, potentially playing different roles in the overall reservoir permeability. The presence of high-angle faults, further corroborated by the 2023 fault model (Figure 14), could contribute to the observed WNW-ESE trend of partially conductive fractures. Open fractures, aligned with the N-S and NE-SW trends, likely represent preferential pathways for geothermal fluids due to their high dip angles and potential connection to larger-scale tectonic structures.

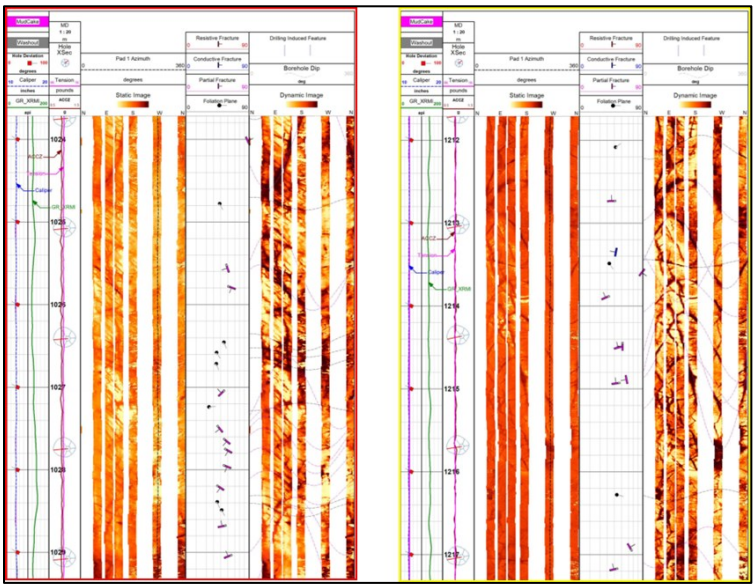

Figure 12. 7-X fractures identified from the image log

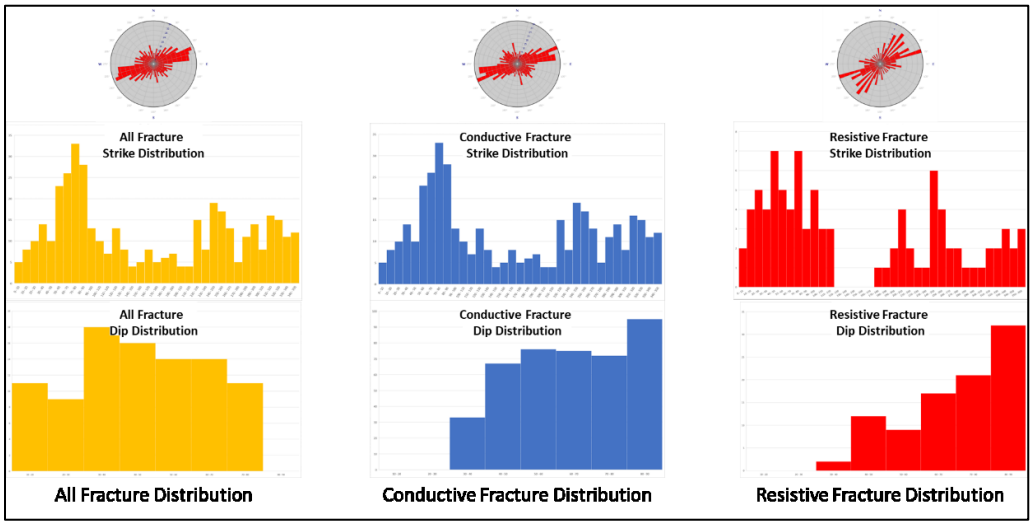

Figure 13. 7-X fracture distribution

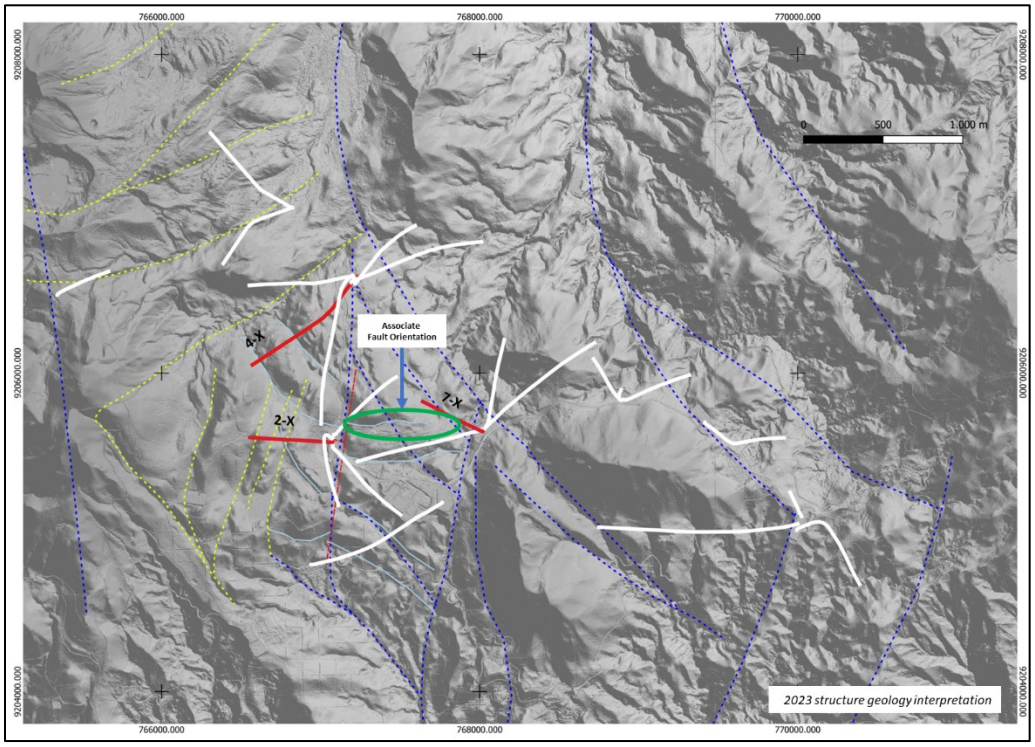

Figure 14. 7-X fault associate

4.4 Completion Test Results in Relation with Permeability

Stationary Spinner responses validated the identified permeable points from moving spinner responses. During flowing test at PTH-G-Stationary spinner data successfully validated permeable points previously identified through moving spinner responses in 4-X and 2-X. During flowing tests, spinner profiles at 100% well opening **(Figure 15)** confirmed permeability at specific depths in both wells.

4-X exhibited permeable zones at 1200 mMD, 1300 mMD, 1650 mMD, 1900 mMD, and 1980 mMD. Notably, only two of these feedzones coincided with identified permeable zones in the borehole image data (Figure 4). These coincident zones correlate with N-S trending fractures, highlighting the crucial role of these fracture orientations in fluid flow.

Similarly, 2-X displayed permeability at 1005 mMD, 1141 mMD, and 1329 mMD, all of which aligned with permeable zones observed in the borehole image data. Interestingly, fractures with N-S and NE-SW trends were associated with these confirmed feedzones, suggesting the importance of both orientations for reservoir fluid flow in this well.

Completion tests are currently ongoing in 7-X, and definitive results regarding feedzone locations will be available upon completion. However, the preliminary data from 4-X and 2-X demonstrates the effectiveness of combining flowing spinner measurements with borehole image analysis for accurately identifying and characterizing productive zones in geothermal wells. This integrated approach can significantly improve future well completion strategies and optimize geothermal resource extraction..

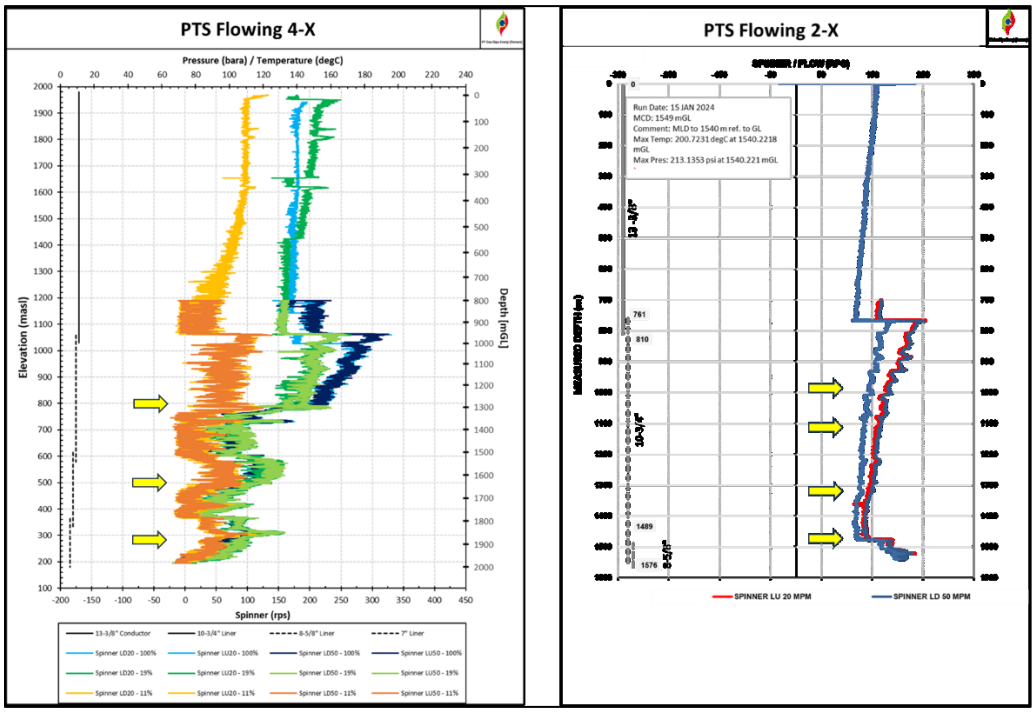

Figure 15. 4-X and 2-X Flowing spinner profiles at 100% well opening

5. CONCLUSION

High-resolution image logs of 4-X, 2-X, and 7-X, corroborated by permeability indications during drilling and production testing, suggest the wells have intersected a mature fault zone within the Patuha geothermal field. This hypothesis strengthens the 2023 structural geology interpretation, indicating that these faults accommodated significant normal and oblique slip movements.

The scattered trend of identified faults, alongside the presence of strike-slip and compartmental faults, suggests a complex, multi-directional fracture system within a narrow area. Additionally, the prevalence of high-dip angles further supports the notion that the Patuha geothermal system is primarily controlled by a strike-slip system.

Our integrated analysis of borehole image log data and well testing results aligns with the established structural model for the Patuha geothermal field (**Figure 3**). This model posits a sinistral strike-slip system dominated by a prominent NE-SW trending main fault. Within this system, en-echelon faults trending NNE-SSW define an extensional duplex that encompasses the geothermal reservoir. Notably, the observed circular fracture patterns within this zone could be attributed to local deformation or non-tectonic events, as suggested by Reski et al. (2023).

On a regional scale, the NE-SW and relative N-S orientations identified in Patuha resonate with the dominant horizontal maximum compressional stress field of Java, trending roughly N-S (Koesmono et al., 1996). This alignment suggests a potential causative link between regional tectonic forces and the development of the strike-slip system governing the Patuha geothermal field. Additionally, the NE-SW and relative N-S trends observed in the fracture networks could be further amplified by local strike-slip deformation processes, as described by Harding (1973).

Drawing upon the conceptual model proposed by Woodcock and Fisher (1986), we interpret the Patuha structure as a sinistral strike-slip system within the larger Patuha area. This system features a main fault trending NE-SW, and an associated extensional duplex defined by en-echelon faults trending NNE-SSW that lie within the geothermal reservoir. Incorporating **Figure 3** further strengthens this interpretation, visually depicting the spatial relationships between the identified fracture networks and the proposed structural model.

ACKNOWLEDGEMENTS

The authors gratefully acknowledge the substantial support of PT. Geo Dipa Energi (Persero) in bringing this study to fruition. We extend our sincere appreciation to the EPDP Division for their invaluable assistance throughout the research process. We would also like to express our gratitude to the Management of PT. Geo Dipa Energi (Persero) for granting permission to publish this work. The successful completion of this study would not have been possible without their dedication and collaboration.

REFERENCES

Ashat, A., et al. "Updating Conceptual Model of Ciwidey-Patuha Geothermal Using Dynamic Numerical Model." IOP Conference Series: Earth and Environmental Science, vol. 254, no. 1, 2019.

Chandra, V. R., et al. "Fault and Structure Study for Field Development Strategy in Patuha Geothermal Project." Proceedings, 47th Workshop on Geothermal Reservoir Engineering, Stanford University, Stanford, CA, 2022.

Elfina, N. S. "Subsurface Geology and Hydrothermal Alteration of the Patuha Geothermal Field, West Java: A Progress Report." ResearchGate, vol. 6, no. 1, 2017, pp. 1-7.

Harding, T.P.: Newport-Inglewood trend, California—An example of wrenching style of deformation, AAPG Bulletin, 57(1), pp.97-116, 1973.

Kusdji, A. F. "Geothermal Exploration in Indonesia: Challenges and Opportunities." 2013. Presentation.

Koesmono. M, Kusnama, and Suwarna. "Peta Geology Lembar Sindangbarang dan Bandarwaru, Jawa, Geology Research and Development Center", 1996.

Pradipta, R. A., et al. "Geology Structure Identification Based on Polarimetric SAR (PolSAR) Data and Field Based Observation at Ciwidey Geothermal Field." IOP Conference Series: Earth and Environmental Science, 2016.

Pulunggono, A., and W. Martodjoyo. Peta Geologi dan Stratigrafi Lembar Bandung (45-12). Pusat Penelitian dan Pengembangan Geologi, 1994.

Reski, E., et al. "Structural Model Update on the Patuha geothermal system, West Java, Indonesia." Proceedings of the 12th ITB International Geothermal Workshop, 2023.

Satyana, A. K. "Peta Struktur Geologi Bandung dan Sekitarnya, Jawa Barat." Jurnal Geologi Indonesia, vol. 4, no. 1, 2007, pp. 1-12.

Stingay, H. R., et al. "Model Tektonik dan Distribusi Sumber Daya Panasbumi di Jawa Barat." Jurnal Sains Teknik Sipil, vol. 15, no. 3, 2010, pp. 85-94.

Woodcock, Nigel H., Fischer, and Mike, "Strike-slip duplexes. Journal of Structural Geology", 8 (7). 725-735, 1986.